ELSEVIER

PII: S0032-3861(97)10101-X

Polymer Vol. 39 No. 15, pp. 3425–3429, 1998

0032-3861/98/$19.00+0.00

Influence of chain extenders and chain end groups on properties of segmented polyurethanes. I. Phase morphology

Yu.V. Savelyev[a,*], E.R. Akhranovich[a], A.P. Grekov[a], E.G. Privalko[a], V.V. Korskanov[a], V.I. Shtompel[a], V.P. Privalko[a], P. Pissis[b] and A. Kanapitsas[b]

[a]*Institute of Macromolecular Chemistry, National Academy of Sciences of Ukraine, 253160 Kyiv, Ukraine*

[b]*National Technical University of Athens, Zografou Campus, 15780 Athens, Greece*

(Accepted 9 September 1997)

Segmented polyurethanes from oligotetramethylene glycol 1000, 4,4′-diphenylmethane diisocyanate and different chain extenders were characterized by specific heat capacity (temperature interval 130–450 K) and small-angle X-ray scattering measurements. A regular macrolattice of uniform-size micro-domains of stiff segments spanning a continuous matrix of soft segments was observed for the sample chain-extended with dihydrazide of isophthalipc acid, DIPA. The distribution of microdomains by sizes remained unchanged, whereas the overall degree of micropahase separation (DMS) increased due to dilution of DIPA and/or blocking of chain ends with crown ether-containing di- and monohydrazides. The distribution of microdomains by sizes broadened, whereas the DMS either remained unchanged or slightly decreased on dilution of DIPA with hydroxyl-containing chain extenders [1,4–di–N–oxy–2,3–bis–(oxymethyl)–quinoxaline and 1,4–butane–diol, respectively].

(Keywords: chain extenders; chain ends; degree of microphase separation)

INTRODUCTION

Segmented polyurethanes (SPU) are the typical representatives of segmented polyblock copolymers in which microphase separation is caused by self-association of stiff (STF) segments. The polyaddition reaction by which STF segments (mostly, aromatic diisocyanates), are bonded to soft (SFT) segments (oligomeric ethers, esters, dienes etc.) via chain extenders (short-chain diols, diamines, dihydrazides and the like) is a stochastic process. This aspect, as well as rather wide molar weight distributions of component segments, is the natural explanation for a broad dispersion of the size of STF microdomains separated from a continuous SFT phase[1–6]. The degree of microphase separation (DMS) is lowest in the case when both STF and SFT fragments are polar and relatively short, and is highest otherwise. For example, the DMS in SPU from poly(propylene glycol) and 4,4′–diphenylmethane diisocyanate (MDI) extended with 1,4–butane diol (BD) was found to decrease, the lower the STF segments content and/or the shorter their length. When the latter decreased below a critical value, the STF segments were assumed to be dissolved within the continuous SFT microphase[7]. The other major factor controlling DMS is the intrinsic flexibility of STF segments: e.g. fairly high DMS in SPU based on polycaprolactone and hexamethylene diisocyanate (HDI) could be reduced to nearly zero by a simple replacement of HDI with a stiffer MDI[8].

In so far as STF microdomains in SPU are usually assumed to be composed of both diisocyanate and chain extender moieties[3–6], it can be anticipated that the latter will affect DMS through its influence on the overall chain flexibility of STF segments. In fact, chain extension by crown ether-containing dihydrazides proved to be an efficient method to control both DMS and physical properties of film-forming SPUs[9,10].

So far, the problem of chain ends had hardly been a point of concern in evaluation of structure–property relationships in SPUs since miscibility of mid-chain fragments and end-groups was tacitly assumed. This assumption, however, may become invalid if chain end-groups will drastically differ from mid-chain units.

According to our preliminary data, use of crown ether-containing and/or heterocyclic compounds as chain extenders and/or chain ends in SPUs can increase the biological activity and complex-forming ability of the latter. Thus, the aim of the present communication is the experimental characterization of the effect of chemical composition of chain extenders and chain end groups on the phase morphology of a novel series of model SPUs.

EXPERIMENTAL

Materials

SPUs of the general structure,

$$H-[-BCE-MDI-TMG-MDI-]-MCE,$$

[where BCE is the bifunctional chain extender (dihydrazide of isophthalic acid, DIPA; dihydrazide of disulfonyl–dibenzo–18– crown–6, DDDC; 1,4–di–N–

* To whom correspondence should be addressed. Tel: 00 380 44 559 40 95; Fax: 00 380 44 552 40 64; e-mail: valery@olinet.isf.kiev.ua

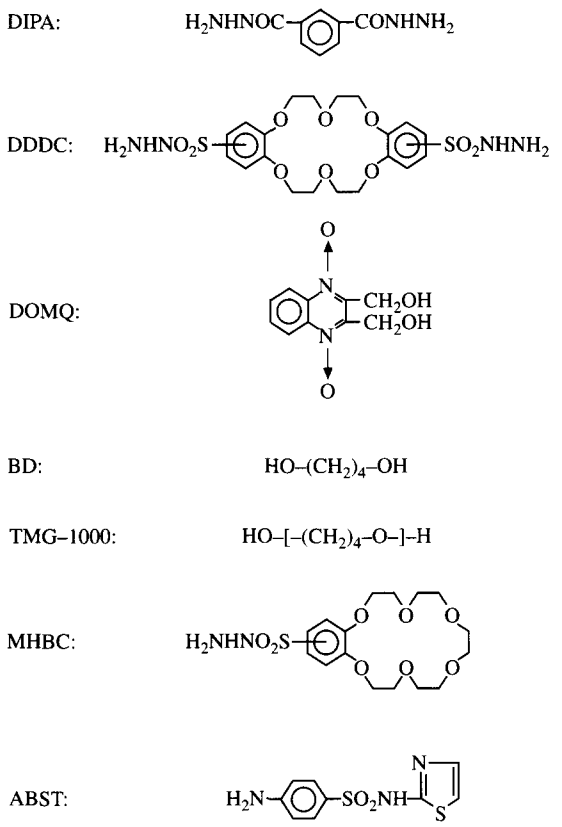

Figure 1 Chemical formulas of chain fragments of SPUs

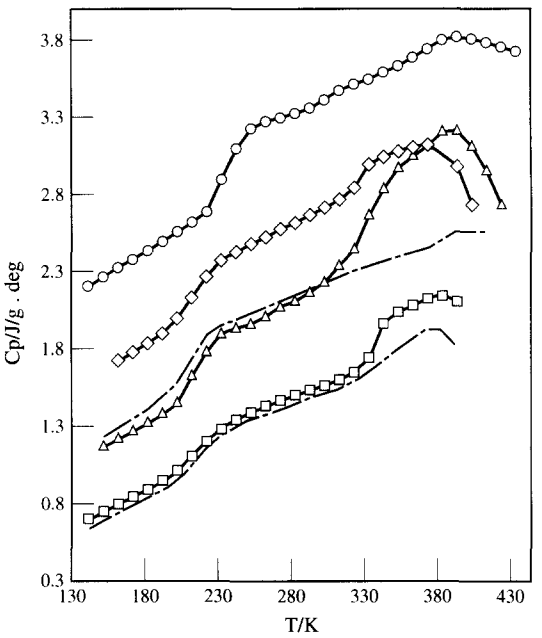

Figure 2 Specific heat capacities of samples 262 (■), 349 (▲), 352 (♦) and 160 (○). Beginning from sample 349, each next curve was shifted upwards by 0.5 J/g deg

oxy–2,3–bis–(oxymethyl)–quinoxaline, DOMQ, and 1,4–butane–diol, BD); TMG-1000 is the oligotetramethylene glycol (molar mass 1000 g/mol), and MCE is the monofunctional chain end (monohydrazide of sulfonyl–benzo–18–crown–6, MHBC, and 2–(n–amino–benzene–sulfamide)–thiazol, ABST)], were prepared by reaction of a BCE with isocyanate end groups of a prepolymer[11,12]. DIPA, DOMQ and ABST were the commercial products used as received; DDDC and MHBC were synthesized according to existing recommendations[11]. Chemical formulas of different chain fragments mentioned above are shown in *Figure 1*. Sample coding, chemical composition of BCE and MCE, densities ρ, and intrinsic viscosities $[\eta]$ (in dimethyl formamide, DMFA), are given in *Table 1*.

Thin films of all SPUs were prepared by casting from DMFA solutions on glass slides and subsequent storage overnight with evacuation to constant weight.

Methods

Specific heat capacity (c_p) in the temperature interval 130–450 K was measured (mean error within the limits 3–4%) by a home-made differential calorimeter with diathermal shells[13] at a heating rate 2 deg/min(sample mass about 0.3–0.4 g).

Small-angle X-ray scattering (SAXS) data were obtained with a KRM type diffractometer (Kratky collimation; primary beam intensity control with a monitoring channel; evacuation of the sample chamber) in the range of scattering

Table 1 Sample coding and chemical composition of chain extenders and chain ends of SPUs

Samplecoding	Chemical composition of SPUs (wt %) Chain extender, chain end						MDI	TMG	UIG[a] (mol %)	$[\eta]$dl/g	ρg/cc
	DIPA	DDDC	DOMQ	BD	MHBC	ABST					
SPU series 1											
160	10.9	—	—	—	—	—	29.7	59.4	—	0.50	1.1370
262	—	27.0	—	—	—	—	24.0	49.0	—	0.34	0.7586
349	5.0	14.0	—	—	—	—	26.0	55.0	—	0.50	—
351	3.0	11.6	—	—	4.4	—	27.0	54.0	15.0	0.35	1.1345
352	3.0	10.0	—	—	7.0	—	27.0	53.0	32.5	0.26	1.1259
SPU series 2											
354	5.0	—	6.0	—	—	—	29.0	60.0	—	0.71	1.1141
355	8.0	—	2.0	—	—	—	29.0	61.0	—	0.68	1.1061
357	8.0	—	1.6	—	—	1.4	29.0	60.0	11.5	0.35	1.1108
358	7.0	2.1	0.9	—	2.0	—	29.0	59.0	10.0	0.58	1.1171
359	7.2	—	—	1.2	—	—	29.9	61.7	—	0.56	1.1430

[a]Unreacted isocyanate groups

Table 2 Selected calorimetric and SAXS data

Sample	W	T_{g1}(K)	Δc_{p1}(J/g deg)	T_{s2}(K)	$\langle L \rangle$(nm)
SPU series 1					
160	0.60	230	0.40	385	10.0
262	0.49	220	0.20	380	19.3
349	0.55	211	0.29	385	14.0
351	0.54	—	—	—	14.0
352	0.53	216	0.24	375	14.0
SPU series 2					
354	0.60	222	0.31	390	10.0
355	0.61	221	0.47	385	10.5
357	0.60	221	0.39	380	11.7
358	0.59	218	0.43	375	11.7
359	0.60	219	0.62	380	9.6

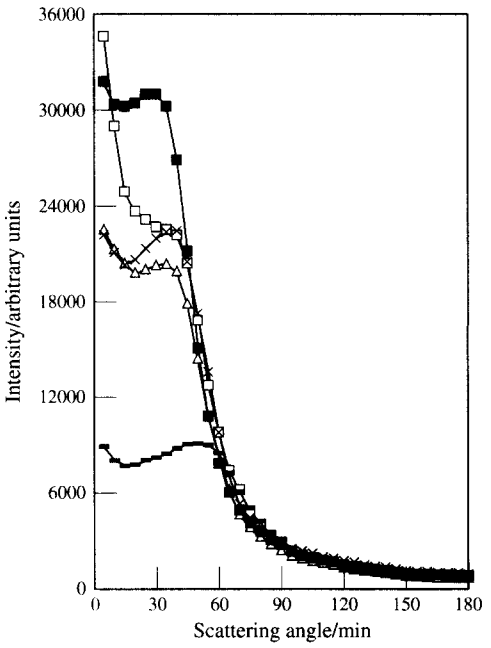

Figure 3 Small-angle X-ray scattering curves for samples 262 (■), 349 (□), 351 (▲), 352 (×) and 160 (— - —)

angles 2q from 5′ to 3° (copper radiation; nickel filtering of the primary beam; step-by-step scanning regime; recording of scattering radiation with a scintillation counter and digital conversion). The geometrical parameters of X-ray beam in the specimen plane and the detector position were chosen so as to satisfy the conditions of an 'infinite' slit collimation (30 mm for the length of the homogeneous portion of X-ray beam and 290 mm for the specimen-detector distance). Thus, it was possible to determine the absolute scattering intensities of SPUs by calibrating the instrument with a standard Kratky sample of Lupolen[14].

RESULTS AND DISCUSSION

SPUs of series 1

Similar to other microphase-separated SPUs[5–10], the most prominent features of the heating thermograms of all studied samples are specific heat capacity jumps (Δc_{p1}) at the glass transition temperatures of SFT-rich microphase (T_{g1}), and endothermic enthalpy relaxations with maxima at T_{s2} (*Figure 2*) which are currently associated with softening of STF-rich microphases. However, as can be seen from *Figure 2* and relevant data collected in *Table 2*, chemical composition of SPU affects temperatures and intensities of both transitions. The highest values of T_{g1} and Δc_{p1} for sample 160 imply the largest content of STF fragments (MDI + DIPA) within the SFT-rich microphase (i.e. the lowest DMS). As a result, the softening endotherm of STF-rich microphase at T_{s2} is the least pronounced.

Dilution of DIPA with DDDC (sample 349) and/or blocking of chain ends with MHBC (sample 352) resulted in the shift of T_{g1} to lower temperatures and in the increase of intensity of T_{s2} relaxations (*Figure 2* and *Table 2*). These data suggest that the content of STF fragments in SFT-rich microphases is decreased, whereas it is increased in STF-rich microphases of these samples compared to sample 160. The apparent increase of DMS for samples 349 and 352 may be tentatively explained by a poor compatibility of crown ether-containing moieties (DDDC and MHBC) with SFT fragments (TMG-1000).

Following this line of reasoning, the highest DMS (i.e. the lowest T_{g1} and the most intensive T_{s2} process) should have been expected for sample 262 with DDDC as the BCE, but this sample differed little from samples 349 and 352 in this respect. Such an apparently anomalous behavior of sample 262 cannot be readily understood at the current stage. It seems pertinent, however, to mention other unique features of this sample:

(1) Persistence of endothermic enthalpy relaxation at T_{s2} in the second heating run; in contrast, this endotherm degenerated to a relatively small specific heat jump in the second heating run of, say, sample 349 (cf. corresponding broken lines in *Figure 2*).
(2) Unusually low values of both specific heat capacity jump Δc_p and density ρ (see *Tables 1 and 2*).

In qualitative terms, the first feature may be attributed to stronger than usual interchain interactions within STF-rich microdomains of sample 262. As a result, the onset of molecular mobility in the rubbery state above T_{s2} would be insufficient to destroy completely the local order within STF-rich microdomains in the first heating run, hence, the occurrence of enthalpy relaxation in the repeated run.

The second feature is more difficult to rationalize. Probably, one should consider a possibility of loose packing (hence, density deficit) and restricted segmental motion (hence, deficit of Δc_p) of a non-negligible portion of SFT fragments sterically immobilized in the boundary layers at the periphery of STF-rich microdomains. It is likely that the same effect is responsible for relatively small values of Δc_p for other samples of this series.

More information on the phase morphology of SPUs can be derived from SAXS data (*Figure 3*). Occurrence of distinct peaks on SAXS curves of all studied SPUs is a direct evidence of the regular, three-dimensional macrolattice of uniform-size STF-rich microdomains spanning the continuous SFT-rich matrix. The relatively narrow dispersion of STF-rich microdomains by sizes suggests random distribution of MDI, DIPA and DDDC moieties within STF fragments of SPU chains, which is consistent with the assumption of equal reactivities of NH-groups in different dihydrazides towards NCO-groups of MDI.

As can be seen from *Figure 3*, the SAXS peaks are shifted to lower scattering angles, the higher the STF content ($1 - W$). The interdomain spacings of the macrolattice (i.e. the corresponding long periods $< L >$ calculated by

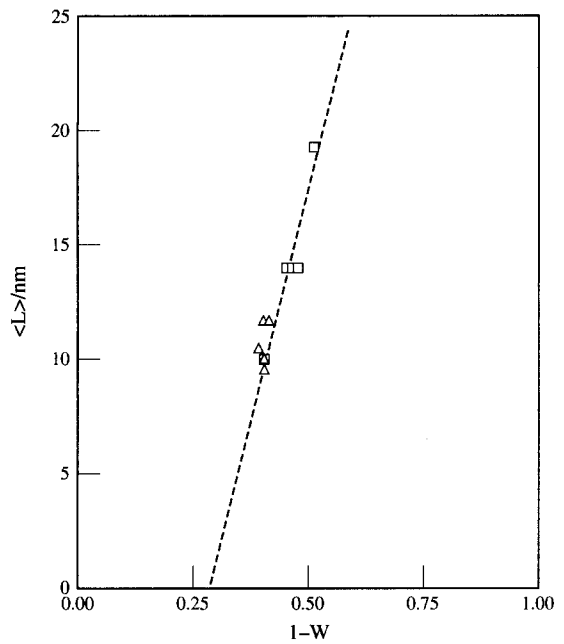

Figure 4 Dependence of long periods on weight content of stiff fragments for samples of series 1 (■) and 2 (▲)

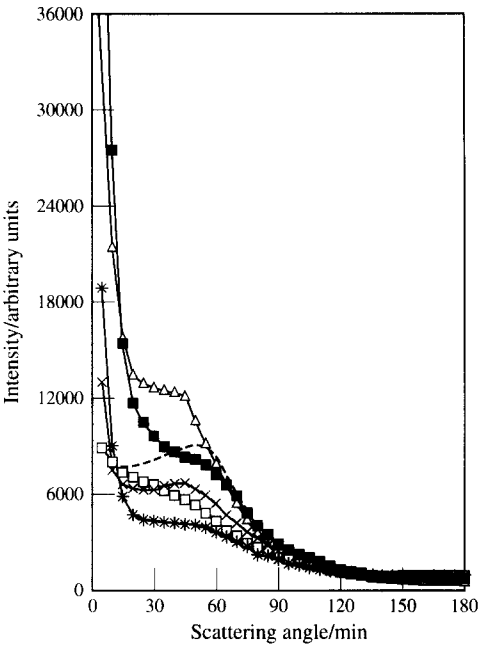

Figure 6 Small-angle X-ray scattering curves for samples 354 (■), 355 (□), 357 (×), 358 (▲), 359 (*) and 160 (— - —)

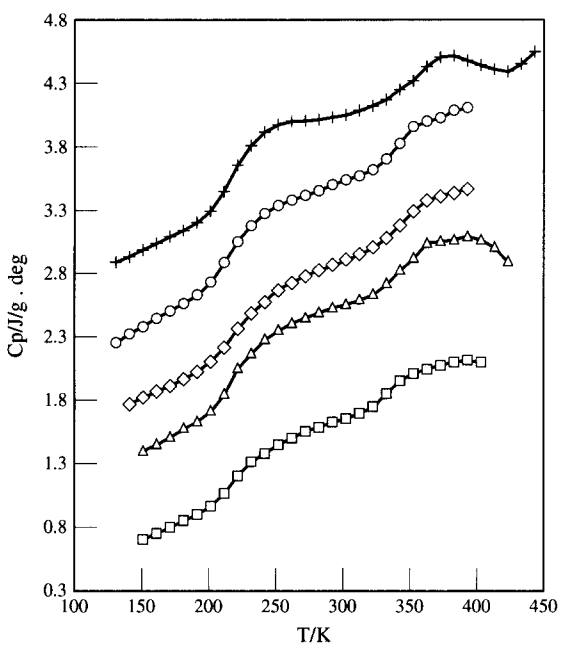

Figure 5 Specific heat capacities of samples 354 (■), 355 (▲), 357 (◇), 358 (○) and 359 (×). Beginning from sample 355, each next curve was shifted upwards by 0.5 J/g deg

Braggs' equation) tend to decrease linearly with $(1 - W)$ (*Figure 4*). The value $(1 - W) = 0.28$ obtained by extrapolation of the straight line in *Figure 4* down to $< L > = 0$ may be regarded as a lower limit of STF content for the onset of microphase separation in our SPUs. In fact, no evidence for SAXS micro-heterogeneity was observed[15] in a structurally similar SPU series from TMG-2000, MDI and BD below $(1 - W) = 0.25$.

As can be seen from *Figure 3*, the intensity of SAXS maxima (i.e. the DMS of SPUs) increases in the order, $262 > 349 = 351 = 352 \gg 160$. This is exactly what can be inferred from our previous analysis of calorimetric data.

The above results may be rationalized as follows. Competition between ether oxygens of SFT and carbonyls of MDI and/or DIPA for interchain hydrogen bonding with proton-donating sites of the latter is responsible for incorporation of a portion of STF fragments in SFT matrix of the initial sample 160, hence, relatively low DMS. Dilution of DIPA with DDDC and/or MHBC decreases the affinity between SFT and STF fragments in samples 349, 351 and 352. Moreover, the tendency of STF fragments for self-association becomes stronger due to long-range electrostatic interactions between negatively-charged cavities of crown ethers and proton-donating sites of STF fragments. These arguments are consistent with the observed increase of the DMS for samples 349, 351 and 352 over that for sample 160, as well as with the highest DMS for sample 262.

SPUs of series 2

All SPU samples of series 2 have similar SFT contents around $X = 0.6$; this may be the reason for similarity of their heating thermograms (*Figure 5*). The main difference between calorimetric data for SPU series 1 and 2 is the systematically higher values of specific heat capacity jumps Δc_{p1} for the latter (*Table 2*). A possible cause of this effect may be the lower overall DMS in SPU of series 2. As a result, enhanced mobility of STF segments at the periphery of STF-rich microdomains will make additional contribution to Δc_{p1}.

The assumption of the lower DMS in SPU of series 2 is qualitatively consistent with systematically smaller intensity of their SAXS peaks (compare *Figures 3, and 6*). Although SAXS curves for SPU of series 2 look quite similar (*Figure 6*), one may still notice that the intensities of SAXS peaks tend to increase in the order $358 > 160 = 354 = 355 = 357 > 359$. Based on these data, one may argue that the DMS is hardly affected by the dilution of DIPA with DOMQ (samples 354, 355) and/or by blocking of chain ends

with ABST (sample 357). As could be anticipated from the foregoing analysis of series 1, the DMS was increased by dilution of DIPA with crown ether-containing DDDC and MHBC (sample 358), whereas the reverse effect was brought about by dilution of DIPA with BD (sample 359).

The composition dependence of SAXS long periods for samples of series 2 is apparently the same as that for series 1 (*Figure 4*), however, judging by the diffuse pattern of SAXS peaks (*Figure 6*), the dispersion of STF-rich microdomains by size for the former is markedly broader. The latter observation may be explained by a considerably lower (about two orders of magnitude[16]) reactivity of OH-groups in DOMQ and BD (compared to NH-groups in DIPA and/or DDDC) towards NCO-groups of MDI. Presumably, SPU chain extension starts by reaction of MDI with a dihydrazide, and it is only after a major part of free NH-groups is consumed that the free OH-groups of DOMQ (BD) will have a chance to react. For this reason, the central blocks of STF fragments will consist primarily of MDI-DIPA-MDI sequences, while the peripheral blocks will be formed by randomly distributed sequences of MDI-DIPA-MDI and MDI-DOMQ(BD)-MDI. As a result, densely-packed sequences of MDI-DIPA-MDI will be concentrated at the cores of STF-rich microdomains, whereas the periphery of the latter will consist of loosely-packed, randomly distributed sequences of MDI-DIPA-MDI and MDI-DOMQ(BD)-MDI. These considerations are qualitatively consistent with both broader dispersion of microdomains by sizes and higher Δc_p for samples of series 2 compared with series 1.

CONCLUSIONS

(1) A regular macrolattice of uniform-size microdomains of stiff segments spanning a continuous matrix of soft segments was observed for the segmented polyurethane from oligotetramethylene glycol 1000 (soft segments) and 4,4′–diphenylmethane diisocyanate, chain-extended with dihydrazide of isophthalipc acid, DIPA (stiff segments).

(2) The distribution of microdomains by sizes remained unchanged, whereas the overall degree of micropahase separation (DMS) increased due to dilution of DIPA and/or blocking of chain ends with crown ether-containing di- and monohydrazides.

(3) The distribution of microdomains by sizes broadened, whereas the DMS either remained unchanged or slightly decreased on dilution of DIPA with hydroxyl-containing chain extenders [1,4–di–N–oxy–2,3–bis–(oxymethyl)–quinoxaline and 1,4–butane–diol, respectively].

ACKNOWLEDGEMENTS

This work was supported by the INTAS project 93-3379-ext, by the NATO Research Fellowship grant for E.G.P., and by the NATO Expert Visit grant HTECH.EV 960944 for V.P.P.

REFERENCES

1. Bonart, R., *Angew. Makromol. Chem.*, 1977, **58/59**, 259.
2. Hu, C. B., Ward, R. S. and Schneider, N. S., *J. Appl. Polym. Sci.*, 1982, **27**, 2167.
3. Miller, J. A., Lin, S. B., Hwang, K. K. S., Wu, K. S., Gibson, P. E. and Cooper, S. L., *Macromolecules*, 1985, **18**, 32.
4. Comargo, R. E., Macosco, C. W., Tirrell, M. and Wellinghoff, S. T., *Polymer*, 1985, **26**, 1145.
5. Privalko, V. P., Usenko, A. A., Vorona, V. V. and Letunovsky, M. P., *J. Polym. Engng*, 1994, **13**, 203.
6. Privalko, V. P., Lipatov, Yu. S., Mirontsov, L. I. and Dashevskii, L. I., *Coll. Polym. Sci.*, 1985, **263**, 691.
7. Koberstein, J. T., Galambos, A. F. and Leung, L. M., *Macromolecules*, 1992, **25**, 6195.
8. Li, Y., Kang, W., Stoffer, J. O. and Chu, B., *Macromolecules*, 1994, **27**, 612.
9. Privalko, V. P., Khaenko, E. S., Khmelenko, G. I., Veselov, V. Ya., Korvyakov, S. G. and Savelyev, Yu. V., *Vysokomol. Soed.*, 1990, **A32**, 1600.
10. Privalko, V. P., Khaenko, E. S., Grekov, A. P. and Savelyev, Yu. V., *Polymer*, 1994, **35**, 1730.
11. Savelyev, Yu. V. and Grekov, A. P., e.a., Patent of Ukraine, no. 94127849.
12. Savelyev, Yu. V., Grekov, A. P., e.a., Patent of Ukraine, No. 95073161, 1995.
13. Privalko, V. P. and Titov, G. V., *Vysokomol. Soed.*, 1979, **A21**, 348.
14. Oranskaya, E. I., Thesis, Institute of Macromolecular Chemistry, National Academy of Sciences of Ukraine, Kyiv, 1991.
15. Abouzahr, S., Wilkes, G. L. and Ophir, Z., *Polymer*, 1982, **23**, 1077.
16. Saunders, J.H. and Frisch, K. C., Polyurethanes, chemistry and technology: Part I. In *Chemistry*. Interscience, New York, 1962.